

## Supporting Information

### **Rational Design of Janus MXene Monolayers as Promising Frameworks for High-performance Sodium Metal Anodes**

Shengbo Wang<sup>a#</sup>, Ziang Ren<sup>a#</sup>, Jinsen Zhang<sup>a</sup>, Shihui Zou<sup>a</sup>, Huadong Yuan<sup>a</sup>, Jianmin Luo<sup>a</sup>, Yujing Liu<sup>a</sup>, Jianwei Nai<sup>a</sup>, Yao Wang<sup>\*ab</sup>, Xinyong Tao<sup>a</sup>

<sup>a</sup> College of Materials Science and Engineering, Zhejiang University of Technology, Hangzhou, 310014, China

<sup>b</sup> Moganshan Research Institute at Deqing County Zhejiang University of Technology, Huzhou, 313000, China

# These authors contributed equally to this work.

\*Corresponding author: [wangyao@zjut.edu.cn](mailto:wangyao@zjut.edu.cn) .

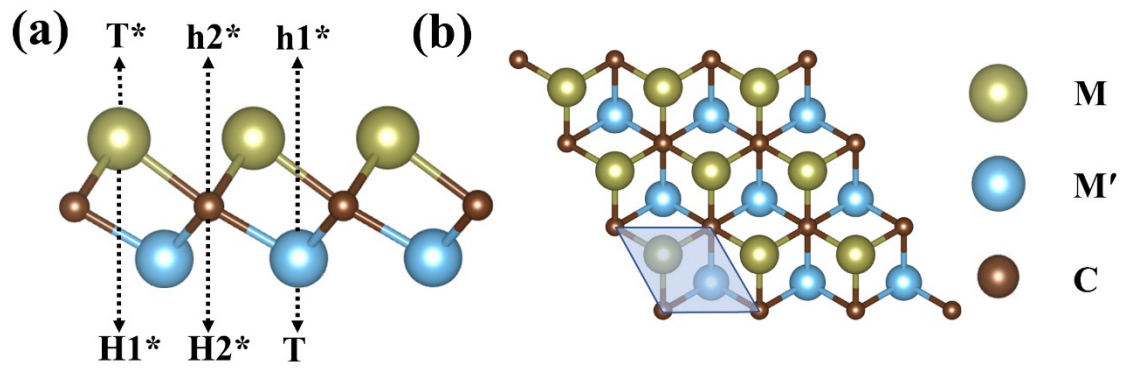


**Fig. S1.** (a) Side view and (b) top view of the MM'C Janus MXene structures. The dark yellow, light blue, and brown spheres represent M, M', and C atoms, respectively.

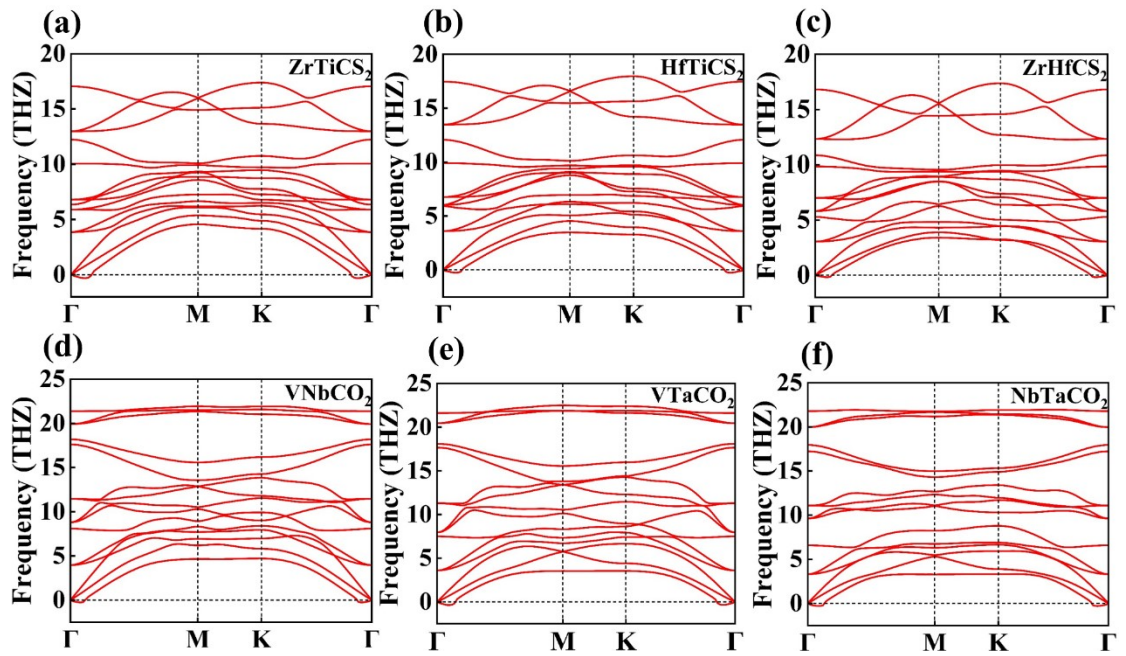


**Fig. S2.** Phonon spectra of (a) ZrTiCS<sub>2</sub>, (b) HfTiCS<sub>2</sub>, (c) ZrHfCS<sub>2</sub>, (d) VNbCO<sub>2</sub>, (e) VTaCO<sub>2</sub>, and (f) NbTaCO<sub>2</sub>.

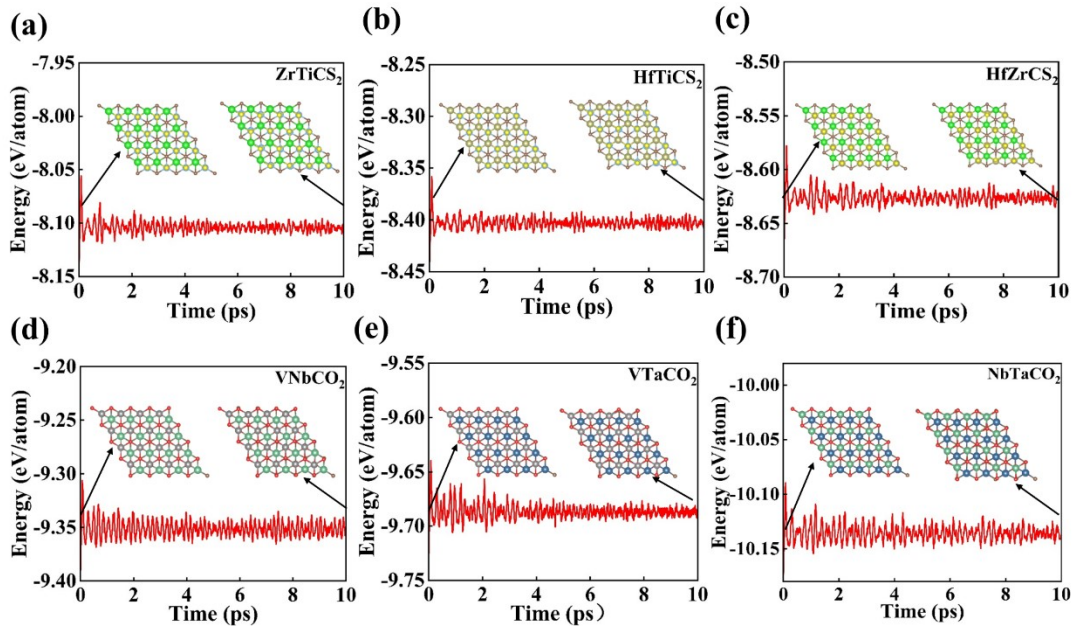


**Fig. S3.** Variation in energy over 10 ps during the AIMD simulation at 300 K of (a)  $\text{ZrTiCS}_2$ , (b)  $\text{HfTiCS}_2$ , (c)  $\text{ZrHfCS}_2$ , (d)  $\text{VNbCO}_2$ , (e)  $\text{VTaCO}_2$ , and (f)  $\text{NbTaCO}_2$  structure.

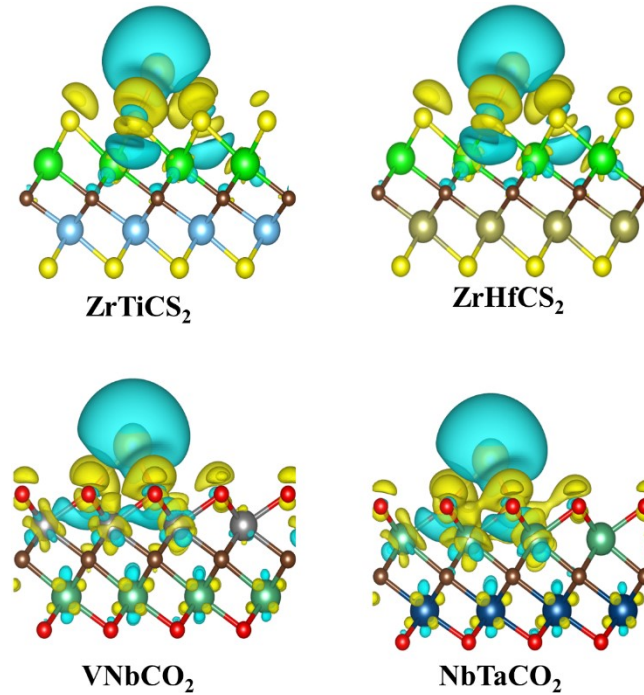


**Fig. S4.** Charge density difference ( $e^- \text{Å}^{-3}$ ) of the Na atom on  $\text{ZrTiCS}_2$ ,  $\text{ZrHfCS}_2$ ,  $\text{VNbCO}_2$ , and  $\text{NbTaCO}_2$ . The isosurface level is set to be  $0.0006 e^- \text{Å}^{-3}$ . The cyan and yellow regions indicate electron depletion and accumulation, respectively.

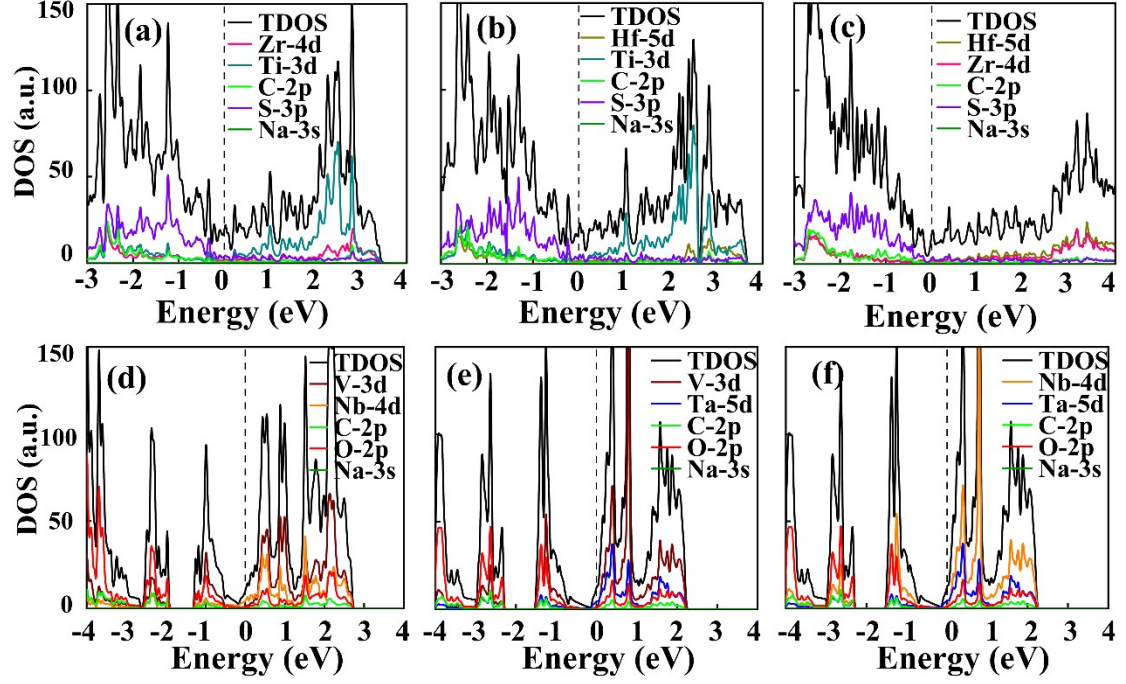


Fig. S5. Single-Na adsorption DOS of (a) ZrTiCS<sub>2</sub>, (b) HfTiCS<sub>2</sub>, (c) HfZrCS<sub>2</sub>, (d) VNbCO<sub>2</sub>, (e) VTaCO<sub>2</sub>, and (f) NbTaCO<sub>2</sub>. The Fermi level is set to zero.

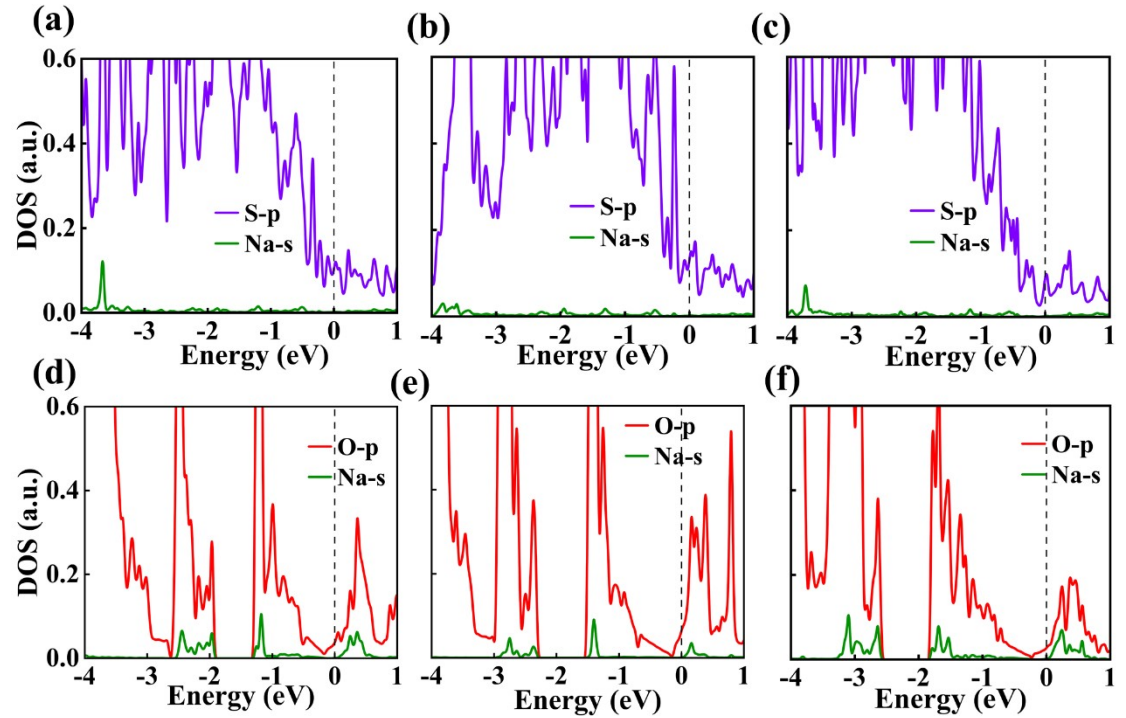
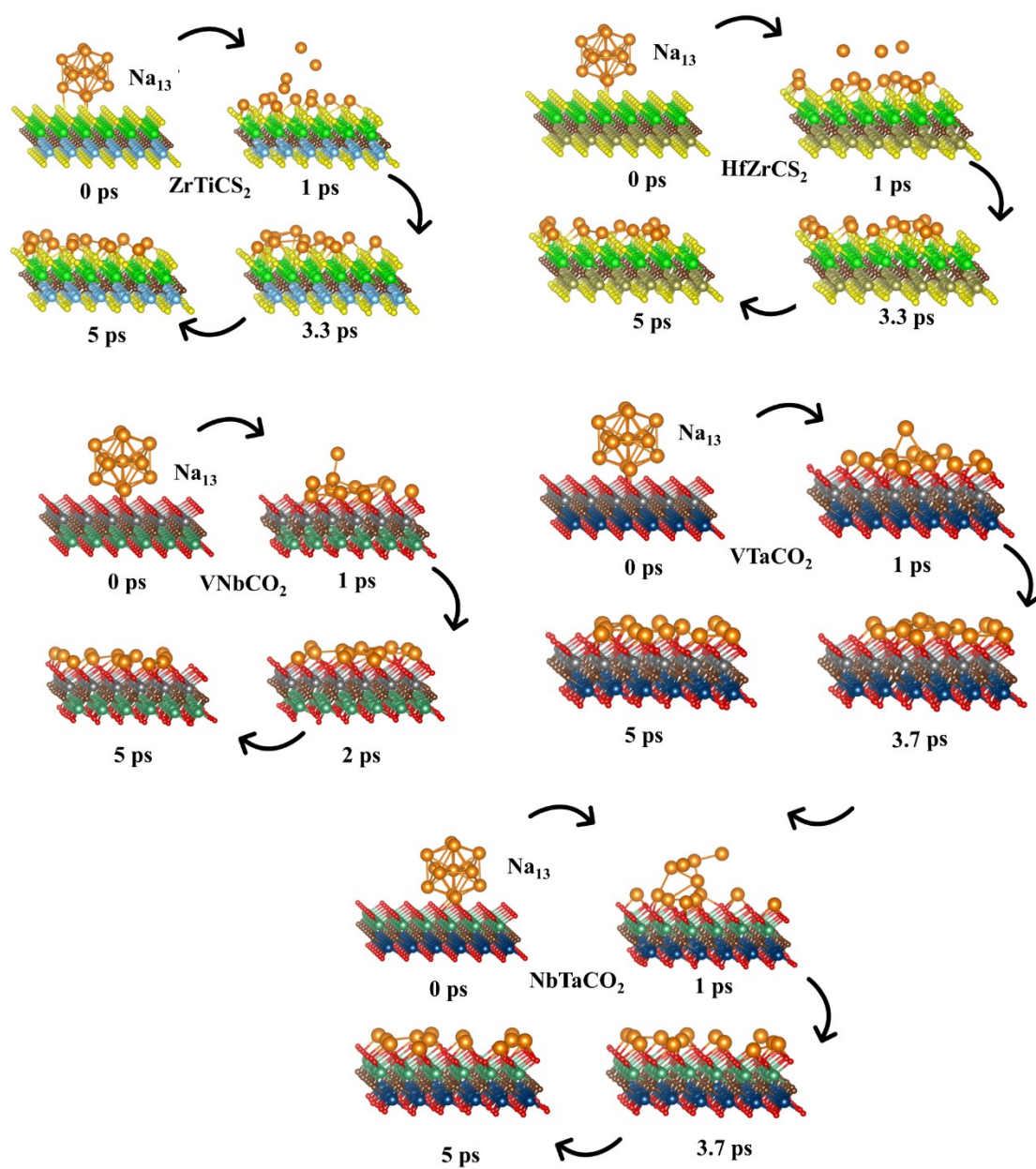
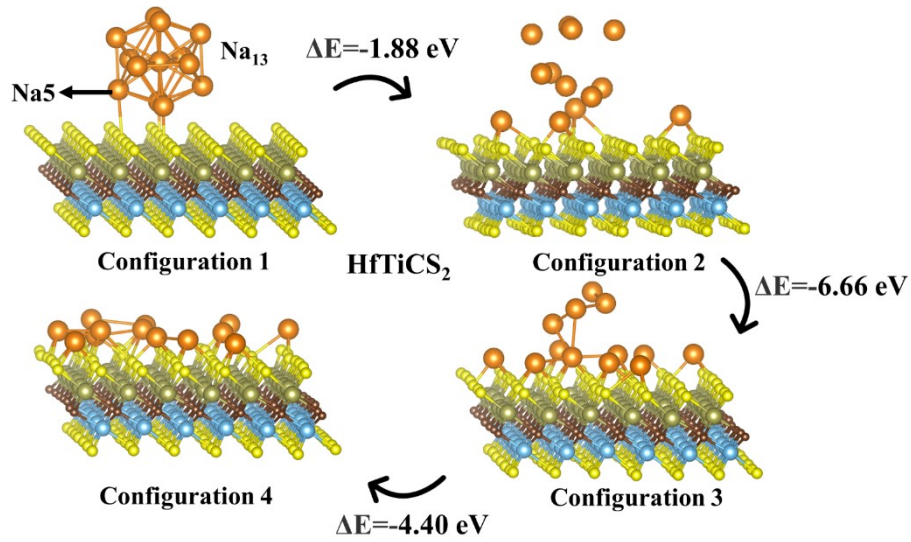


Fig. S6. (a-c) PDOS of the adsorbed Na atom and its surrounding S atom in ZrTiCS<sub>2</sub>, HfTiCS<sub>2</sub>, and HfZrCS<sub>2</sub>, (d-f) PDOS of the adsorbed Na atom and its surrounding O atom in VNbCO<sub>2</sub>, VTaCO<sub>2</sub>, and NbTaCO<sub>2</sub>. The Fermi level is set to zero.



**Fig. S7.** Snapshots of AIMD simulations of  $\text{Na}_{13}$  on  $\text{ZrTiCS}_2$ ,  $\text{HfZrCS}_2$ ,  $\text{VNbCO}_2$ ,  $\text{VTaCO}_2$ , and  $\text{NbTaCO}_2$  Janus MXene at 300 K.



**Fig. S8.** The four-state structure of the  $\text{Na}_{13}$  cluster on the  $\text{HfTiCS}_2$  Janus MXene surface during the 3D-to-2D transition at 300 K.

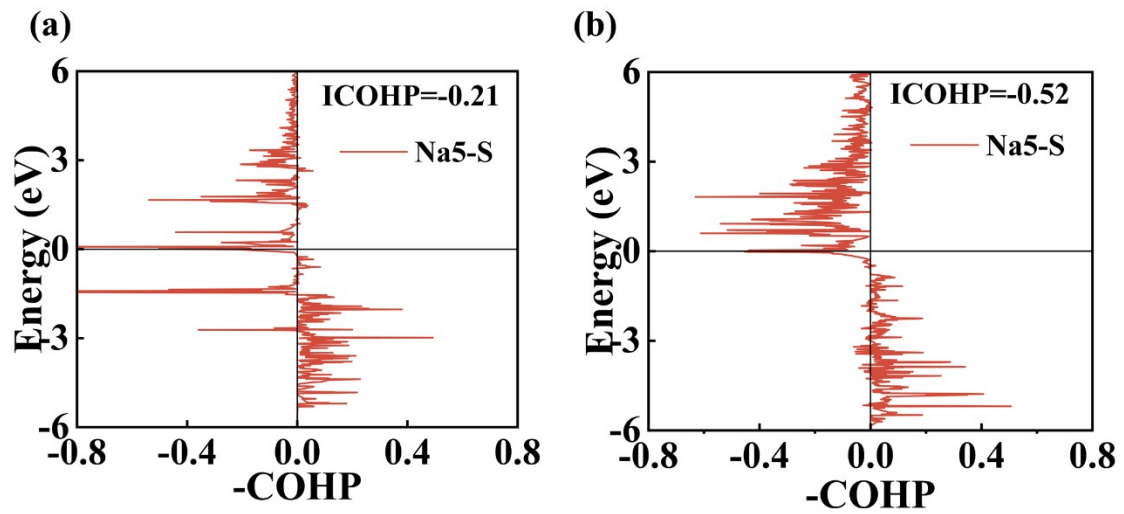


**Fig. S9.** (a) The COHP of Na5 atom within the  $\text{Na}_{13}$  clusters in interacting with surface S atoms in configuration 1. (b) The COHP of Na5 atom within the  $\text{Na}_{13}$  cluster in interacting with surface S atoms in configuration 4.

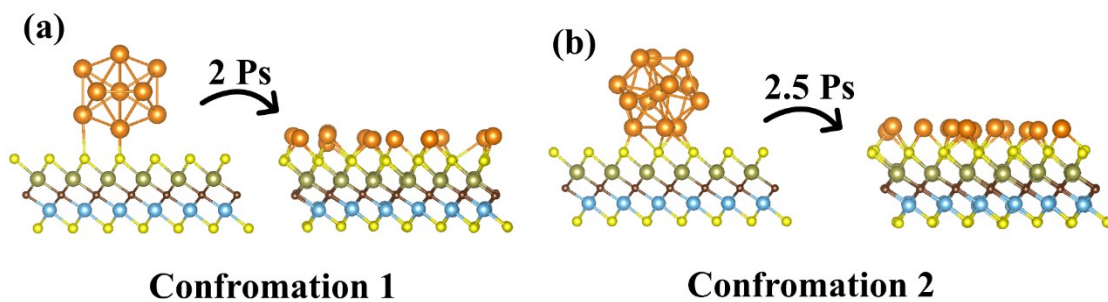


**Fig. S10.** Snapshots of AIMD simulations of different  $\text{Na}_{13}$  conformations on  $\text{HfTiCS}_2$  Janus MXene at 300 K. (a) Conformation 1. (b) Conformation 2.

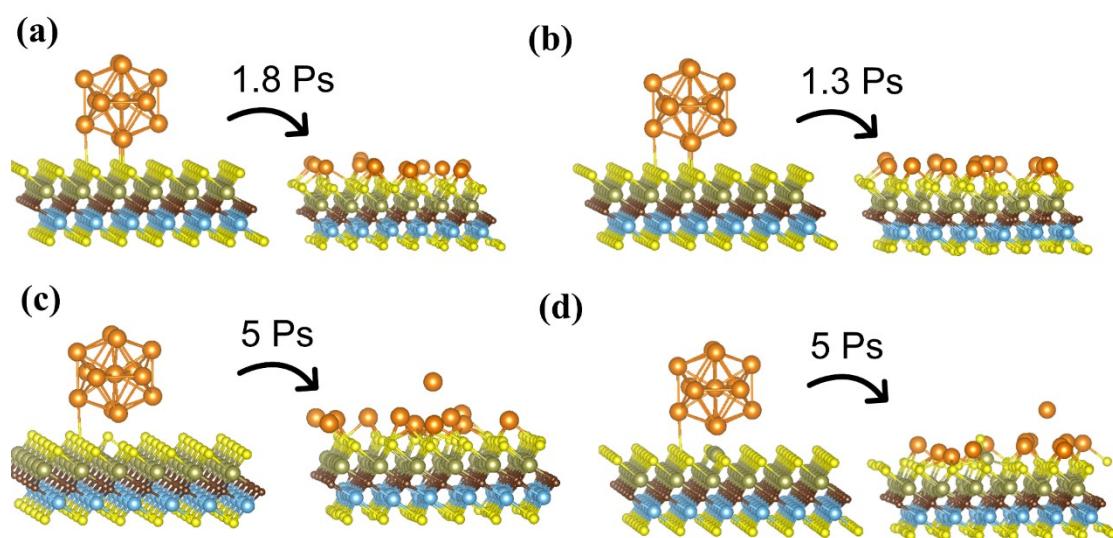


**Fig. S11.** (a) and (b) Snapshots of AIMD simulations of  $\text{Na}_{13}$  on  $\text{HfTiCS}_2$  Janus MXene at 400 K and 500K. (c) and (d) Snapshots of AIMD simulations of  $\text{Na}_{13}$  on vacancy-defect and doped-defect  $\text{HfTiCS}_2$  Janus MXene at 300 K

**Table S1.** Lattice parameter, lengths of M–C ( $d_{M-C}$ ), M'–C ( $d_{M'-C}$ ), M–S ( $d_{M-S}$ ), and M'–S ( $d_{M'-S}$ ) bonds of all MM'CS<sub>2</sub>, M<sub>2</sub>CS<sub>2</sub>, and M<sub>2</sub>'CS<sub>2</sub> MXenes are shown.

	Lattice (Å)	$d_{M-C}$ (Å)	$d_{M'-C}$ (Å)	$d_{M-S}$ (Å)	$d_{M'-S}$ (Å)
ZrTiCS <sub>2</sub>	3.31	2.33	2.26	2.53	2.41
HfTiCS <sub>2</sub>	3.29	2.31	2.26	2.50	2.41
ZrHfCS <sub>2</sub>	3.43	2.4	2.37	2.53	2.41
Ti <sub>2</sub> CS <sub>2</sub>	3.16	2.19	/	2.40	/
Zr <sub>2</sub> CS <sub>2</sub>	3.45	2.4	/	2.53	/
Hf <sub>2</sub> CS <sub>2</sub>	3.41	2.37	/	2.51	/

**Table S2.** Lattice parameter, lengths of M–C ( $d_{M-C}$ ), M'–C ( $d_{M'-C}$ ), M–O ( $d_{M-O}$ ), and M'–O ( $d_{M'-O}$ ) bonds of All MM'CO<sub>2</sub>, M<sub>2</sub>CO<sub>2</sub>, and M<sub>2</sub>'CO<sub>2</sub> MXenes are shown.

	a (Å)	$d_{M-C}$ (Å)	$d_{M'-C}$ (Å)	$d_{M-O}$ (Å)	$d_{M'-O}$ (Å)
VNbCO <sub>2</sub>	2.98	2.08	2.14	2.03	2.07
VTaCO <sub>2</sub>	2.99	2.09	2.13	2.03	2.08
NbTaCO <sub>2</sub>	3.08	2.22	2.15	2.11	2.1
V <sub>2</sub> CO <sub>2</sub>	2.88	2.04	/	1.95	/
Nb <sub>2</sub> CO <sub>2</sub>	3.10	2.19	/	2.09	/
Ta <sub>2</sub> CO <sub>2</sub>	3.12	2.19	/	2.1	/

**Table S3.** Binding energies (unit: eV) of Na-adatom on Janus MXenes at different sites. The largest binding energies were highlighted.

	E <sub>T1</sub>	E <sub>H1</sub>	E <sub>H2</sub>	E <sub>T2</sub>	E <sub>h1</sub>	E <sub>h2</sub>
ZrTiCS <sub>2</sub>	-2.08	-2.62	<b>-2.63</b>	-1.98	-2.50	-2.50
HfTiCS <sub>2</sub>	Unstable	-2.47	<b>-2.51</b>	-1.94	-2.49	-2.46
ZrHfCS <sub>2</sub>	Unstable	-2.47	<b>-2.52</b>	-1.89	-2.43	-2.46
	E <sub>T3</sub>	E <sub>H3</sub>	E <sub>H4</sub>	E <sub>T4</sub>	E <sub>h3</sub>	E <sub>h4</sub>
VNbCO <sub>2</sub>	-2.59	<b>-3.09</b>	-3.01	-1.53	-1.93	-2.01
VTaCO <sub>2</sub>	-2.29	<b>-2.79</b>	-2.71	-0.88	-1.27	-1.35
NbTaCO <sub>2</sub>	-2.06	<b>-2.54</b>	-2.43	-0.88	-1.25	-1.34



**Table S4.** The alteration in the charge state of M (M') atom following the formation of S-terminated MXenes

	$\Delta Q_m$ ( e )	$\Delta Q_{m'}$ ( e )
ZrTiCS <sub>2</sub>	-1.83	-1.63
HfTiCS <sub>2</sub>	-1.89	-1.62
ZrHfCS <sub>2</sub>	-1.88	-1.90
Ti <sub>2</sub> CS <sub>2</sub>	-1.64	/
Zr <sub>2</sub> CS <sub>2</sub>	-1.89	/
Hf <sub>2</sub> CS <sub>2</sub>	-1.92	/

**Table S5.** The alteration in the charge state of M (M') atom following the formation of O-terminated MXenes

	$\Delta Q_m$ ( e )	$\Delta Q_{m'}$ ( e )
VNbCO <sub>2</sub>	-1.66	-2.07
VTaCO <sub>2</sub>	-1.66	-2.16
NbTaCO <sub>2</sub>	-1.85	-2.21
V <sub>2</sub> CO <sub>2</sub>	-1.75	/
Nb <sub>2</sub> CO <sub>2</sub>	-2.05	/
Ta <sub>2</sub> CO <sub>2</sub>	-2.13	/

**Table S6.** Calculated electric charge transferred ( $\Delta Q$ ) from Na-atom to Janus MXenes surface.

	$\Delta Q_m$ ( e )
ZrTiCS <sub>2</sub>	0.886
HfTiCS <sub>2</sub>	0.885
ZrHfCS <sub>2</sub>	0.882
VNbCO <sub>2</sub>	0.911
VTaCO <sub>2</sub>	0.910
NbTaCO <sub>2</sub>	0.909

**Table S7.** The distance (H) between the adsorbed Na atom and the M transition metal layer in various Janus MXenes

	H (Å)
VNbCO <sub>2</sub>	2.750
VTaCO <sub>2</sub>	2.760
NbTaCO <sub>2</sub>	2.830
ZrTiCS <sub>2</sub>	3.430
HfTiCS <sub>2</sub>	3.540
ZrHfCS <sub>2</sub>	3.510

**Table S8.** Binding energy (eV) of Na clusters with different structures and Janus MXenes

	Configuration 1	Configuration 2	Configuration 3	Configuration 4
ZrTiCS <sub>2</sub>	-0.13	-0.72	-1.19	-1.21
HfTiCS <sub>2</sub>	-0.12	-0.77	-1.11	-1.12
ZrHfCS <sub>2</sub>	-0.11	-0.78	-1.18	-1.20
VNbCO <sub>2</sub>	-0.20	-0.83	-1.13	-1.23
VTaCO <sub>2</sub>	-0.22	-0.92	-1.11	-1.12
NbTaCO <sub>2</sub>	-0.14	-0.78	-0.89	-0.92

**Table S9.** The average charge ( $\Delta Q$ ) transferred to the surface of Janus MXenes by a single Na atom within the Na<sub>13</sub> cluster.

	Configuration 1	Configuration 2	Configuration 3	Configuration 4
ZrTiCS <sub>2</sub>	0.22	0.47	0.59	0.73
HfTiCS <sub>2</sub>	0.21	0.42	0.55	0.77
ZrHfCS <sub>2</sub>	0.21	0.45	0.60	0.82
VNbCO <sub>2</sub>	0.22	0.42	0.61	0.76
VTaCO <sub>2</sub>	0.22	0.48	0.63	0.74
NbTaCO <sub>2</sub>	0.22	0.41	0.52	0.74